

70 nm gate-length THz InP-based $\text{In}_{0.7}\text{Ga}_{0.3}\text{As}/\text{In}_{0.52}\text{Al}_{0.48}\text{As}$ HEMT With f_{max} of 540GHz

Lisen Zhang, Zhihong Feng, Dong Xing, Shixiong Liang, Junlong Wang, Guodong Gu, Yuangang Wang, and Peng Xu*

National Key Laboratory of Application Specific Integrated Circuit, Hebei Semiconductor Research Institute, Shijiazhuang 050051, China, zhls1209@163.com, ga917vv@126.com, d.xing@126.com, wialliam@163.com, tjuwangjunlong@126.com, ggd1312@163.com, wyg123006@126.com, maxuanxupeng@126.com

Abstract

A 70 nm gate-length $\text{In}_{0.7}\text{Ga}_{0.3}\text{As}/\text{In}_{0.52}\text{Al}_{0.48}\text{As}$ InP-based high electron mobility transistor (HEMT) was successfully fabricated with a gate width of $2 \times 20 \mu\text{m}$ and source-drain space of $2 \mu\text{m}$. The T-shaped gate with a stem height of 200nm is fabricated to minimize parasitic capacitance. The fabricated devices exhibited a maximum drain current density of 720 mA/mm ($V_{\text{GS}}=0.2\text{V}$) and a maximum peak extrinsic-transconductance of 1600 mS/mm. The current gain extrinsic cutoff frequency f_T and the maximum oscillation frequency f_{max} were 310 and 540 GHz, respectively. The HEMTs are promising for use in THz-wave integrated circuits.

1. Introduction

The Terahertz (THz) frequency range from 0.3 to 3 THz has tremendous potential for various applications such as radio astronomy, medicine, communication, security and defence [1-6]. Compared to microwave and millimeter wave, THz radiation, which is in the range of 0.1mm to 1mm, has several particular advantages such as high resolution, ultra wideband, and high security. Wireless communication systems are expanding fast and the demand for data rates is growing. Due to the huge available multiple gigahertz (GHz) broad bandwidths, THz waves offer the possibility for wireless transmission of high data rates, which can help satisfy the ever-growing demand for data rates [3,4]. Due to severe atmospheric attenuation, in the past decade, Terahertz technology has been mainly driven by applications in astronomy. Compared with microwave and millimeter-wave bands, basic research and applications in the THz band are still in infancy.

The developments of THz communication systems have been slow because very high free space losses occur in the THz band and the achievable output power is fairly limited to only a few mW [7]. As a result, THz transistors and amplifiers have been researched widely and made great progress. InP-based high-electron mobility transistors (HEMTs) have been proved to be the most promising devices that can operate in the THz frequency range, because of high electron mobilities, high saturation velocities, and high sheet electron densities in the channel. Recent reports of record high-frequency characteristics as assessed by the current-gain cutoff frequency f_T and the maximum oscillation frequency f_{max} of InP-based HEMTs, have been published. Current records for f_T and f_{max} are 644 GHz [8] and 1.2 THz with a 35nm gate-length technology [9], respectively.

In this paper, the design, fabrication, and characteristics of 70 nm gate-length InP-based HEMTs were described. Source and drain ohmic contacts were formed with non-alloyed Ni/Ge/Au. The T-shaped gate with a stem height of 200nm is fabricated to minimize parasitic capacitance. The frequency characteristics of $f_T = 310$ GHz, $f_{\text{max}} = 540$ GHz, and $G_{\text{m,max}} = 1600$ mS/mm of the device were demonstrated.

2. Device fabrication

Pseudomorphic HEMT epitaxial layers were grown on semi-insulating (100) InP substrate by metalorganic chemical vapor deposition (MOCVD). The schematic of the structure is shown in Fig. 1 and given as follows. These layers resemble a typical InP HEMT layer structure, with semi-insulating InP substrate, $\text{In}_{0.52}\text{Al}_{0.48}\text{As}$ buffer layer, pseudomorphic 10-nm $\text{In}_{0.7}\text{Ga}_{0.3}\text{As}$ channel, 13-nm $\text{In}_{0.52}\text{Al}_{0.48}\text{As}$ barrier, 5-nm InP etching stop layer, and a 20-nm bulk-doped $\text{In}_{0.53}\text{Ga}_{0.47}\text{As}$ cap layer. A Si doping plane was inserted in the Schottky layer to supply electrons for current conduction. Hall measurements on this structure, after removing the cap layer, showed a two-dimensional electron gas (2DEG) sheet density of $2.6 \times 10^{12} \text{ cm}^{-2}$ and a mobility of $10300 \text{ cm}^2/\text{V}\cdot\text{s}$ at room temperature (RT).

n ⁺ InGaAs Cap layer
InP etching stop layer
In _{0.52} Al _{0.48} As barrier
----- Si doping plane -----
In _{0.52} Al _{0.48} As spacer
In _{0.7} Ga _{0.3} As channel
In _{0.52} Al _{0.48} As buffer
InP substrate

Fig. 1 Schematic of the material structure of InP HEMT material layer structure.

The Mesa isolation was done by means of a phosphorus acid based wet chemical etching to expose the In_{0.52}Al_{0.48}As buffer layer. Source and drain ohmic contacts were formed with non-alloyed Ni/Ge/Au with a spacing of 2μm. Transmission line method (TLM) measurements revealed the contact resistance of 0.067Ω·mm and the specific contact resistivity of 5.82×10⁻⁷Ω/cm² on linear TLM patterns, which could be further reduced using improved process.

A conventional tri-layer resist (ZEP/PMGI/ZEP) was used for EB lithography. The T-shaped gate with a Ti/Pt/Au (20/30/250 nm) metal stack was fabricated with a stem height of 200nm to minimize parasitic capacitance. Before gate metallization, a two-step recess process was used to expose an InAlAs barrier. Figure 2 shows SEM image of the 70-nm T-shaped gate.



Fig. 2 SEM image of 70-nm InP PHEMT gate

3. Results and discussion

The current-voltage characteristics of 2×20μm devices measured at room temperature are shown in Figure 3. The gate-source voltage (V_{GS}) is decreased from (top) 0.2V to (bottom) -0.8V in steps of -0.2V. Good pinch-off characteristics were observed at V_{GS} =-0.8V. The drain current rises with the increase of drain-source voltage (V_{DS}), which is attributed to impact ionization because of the narrow band-gap of In_{0.7}Ga_{0.3}As channel. Figure 4 shows the V_{GS} dependence on the I_{DS} and extrinsic transconductance (G_m) of the HEMT when biased at V_{DS} of 1V. The device shows a threshold voltage (V_{TH}) of about -0.6V. The drain-source current (I_{DS}) reached about 720mA/mm at V_{DS} =1.0V and V_{GS} =0.2V. An extrinsic maximum transconductance (G_{m_max}) of 1600mS/mm is obtained at V_{DS} =1V and V_{GS} =-0.5V, which is attributed to shorter gate-length and higher mobility of In_{0.7}Ga_{0.3}As channel material.

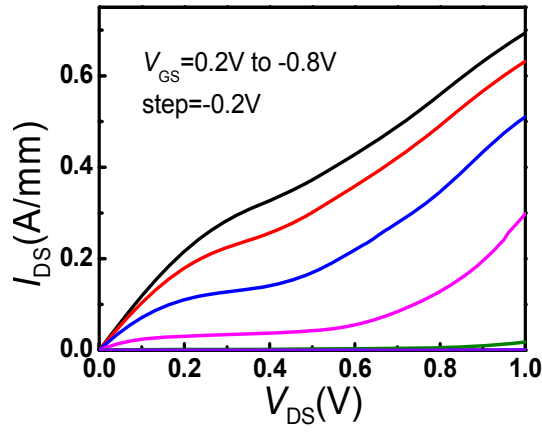


Fig. 3 Output characteristics of the InGaAs/InAlAs HEMT

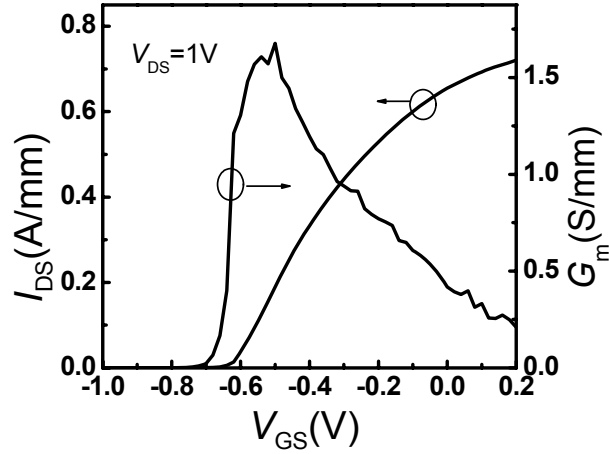


Fig. 4 Transfer characteristics of the HEMT

On-wafer small-signal RF performances of devices were characterized with an Agilent vector network analyzer, which swept from 75 to 110 GHz in 0.5 GHz steps. S-parameter measurements for open and short pads were also performed on the same wafer in order to calibrate the parasitic capacitance and inductance components related to the pad metals. The current gain H_{21} and the maximum stable gain/maximum available gain (MSG/MAG) of devices was derived from measured S-parameters as a function of frequency. The small signal characteristic of the device with a 70 nm gate length and $2 \times 20 \mu\text{m}$ gate width is shown in Fig. 5. A cut-off frequency f_T of 310 GHz was obtained at $V_{GS} = -0.4$ V and $V_{DS} = 1.2$ V by extrapolating H_{21} , and a maximum oscillation frequency f_{max} of 540 GHz was achieved by extrapolating MAG/MSG using a least-square fitting with a -20 dB/decade slope.

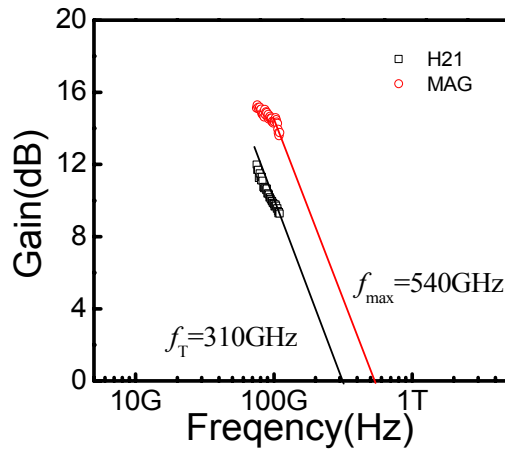


Fig.5. Small signal characteristics of an InGaAs/InAlAs PHEMT device with a 70nm gate length and a $2 \times 20 \mu\text{m}$ gate width

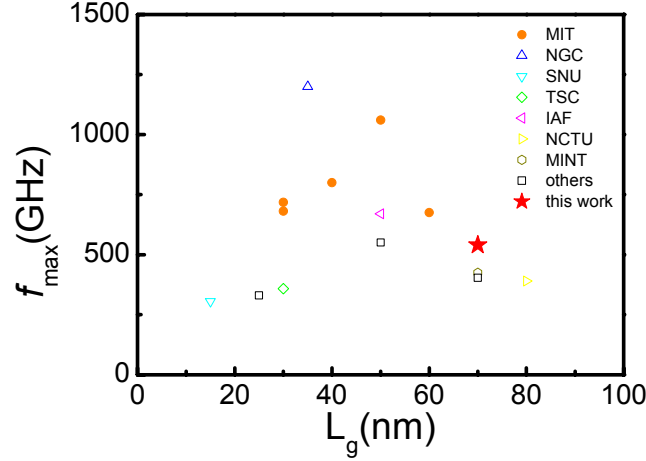


Fig.6. f_{max} as a function of L_g for reported InGaAs and InAs HEMTs in the literature

Fig. 6 shows f_{max} as a function of L_g for sub-100 nm InGaAs and InAs HEMTs. The obtained f_{max} value in our devices is higher than most of ever reported in a HEMT above $L_g = 70$ nm. The excellent frequency performances promise the possibility of THz-wave applications, especially for W-band millimeter-wave devices and circuits. More outstanding device performances would be obtained by optimizing the material structure, reducing the gate length of T-gate and the space of drain-to-source.

4. Conclusion

In summary, 70 nm gate-length InP-based $\text{In}_{0.7}\text{Ga}_{0.3}\text{As}/\text{In}_{0.52}\text{Al}_{0.48}\text{As}$ HEMTs have been fabricated. DC and RF performances are measured. The maximum drain current density and maximum peak extrinsic transconductance were 720 mA/mm and 1600 mS/mm, respectively. At the same time, a current gain cut-off frequency of 310 GHz and a maximum oscillation frequency of 540 GHz were obtained. Further device fabricated technology can be used to improve device DC and RF performances, such as reducing the source-drain space, gate-length and so on.

5. References

1. P. H. Siegel, "THz for space: The golden age," 2010 IEEE MTT-S International Microwave Symposium Digest, 2010, pp. 23-28.
2. S. J. Oha, Y. M. Huha, S. Haamb, J. S. Suha, and J. H. Sonc, "Medical Application of THz Imaging Technique," 37th International Conference on Infrared, Millimeter, and Terahertz Waves, 2012, pp. 1-3.
3. R. Piesiewicz, T. Kleine-Ostmann, N. Krumbholz, D. Mittleman, M. Koch, J. Schoebel, and T. Kürner, "Short-Range Ultra-Broadband Terahertz Communications: Concepts and Perspectives," IEEE Antennas and Propagation Magazine, vol. 49, no. 6, 2007, pp. 24-39.
4. H. Song and T. Nagatsuma, "Present and future of terahertz communications," IEEE Trans. TeraHz. Sci. Technol., vol. 1, no. 1, Sep. 2011, pp. 256-263.
5. N. Palka, M. Szustakowski, M. Kowalski, T. Trzcinski, R. Ryniec, M. Piszczek, W. Ciurapinski, M. Zyczkowski, P. Zagrajek, and J. Wrobel, "THz Spectroscopy and Imaging in Security Applications," 19th International Conference on Microwaves, Radar and Wireless Communications, Warsaw, Poland, 2012, pp. 265-270.
6. H. B. Liu, H. Zhong, N. Karpowicz, Y. Q. Chen, and X. C. Zhang, "Terahertz Spectroscopy and Imaging for Defense and Security Applications," Proceedings of the IEEE, vol. 95, no. 8, August 2007, pp. 1514-1527.
7. L. A. Samoska, "An Overview of Solid-State Integrated Circuit Amplifiers in the Submillimeter-Wave and THz Regime," IEEE Transactions on Terahertz Science and Technology, vol. 1, no. 1, September 2011, pp. 9-24.
8. D. H. Kim and J. A. del Alamo, "30-nm InAs PHEMTs With $f_T = 644$ GHz and $f_{max} = 681$ GHz," IEEE Electron Device Letters, vol. 31, no. 8, August 2010, pp.806-808.
9. R. Lai, X. B. Mei, W. R. Deal, W. Yoshida, Y. M. Kim, P. H. Liu, J. Lee, J. Uyeda, V. Radisic, M. Lange, T. Gaier, L. Samoska, and A. Fung, "Sub 50 nm InP HEMT device with f_{max} greater than 1 THz," IEDM, 2007, pp. 609-612.